Next Materials 8 (2025) 100789

Contents lists available at ScienceDirect

Next Materials

journal homepage: www.sciencedirect.com/journal/next-materials

Research article

Magnetic and levitation properties of YBCO/polymer composite drop-casting films

Beatriz Lucas [a,b], Miguel Brito [a], Canan Aksoy [c], Bakiye Cakir [d], Elvan Coşkun [e], Ali Gencer [e,f], Anabela Pronto [b,g], Isabel Ferreira [a,*]

[a] CENIMAT|i3N, Department of Materials Science, School of Science and Technology, NOVA University Lisbon, Caparica, Portugal
[b] Electrical and Computer Engineering Department, School of Science and Technology, NOVA University Lisbon, Caparica, Portugal
[c] Electronics and Communication Engineering, Faculty of Technology, Karadeniz Technical University, Trabzon 61830, Turkiye
[d] Vocational School of Health Services, Artvin Çoruh University, Artvin 08000, Turkiye
[e] Ankara University, Superconductor Technologies Application and Research Center, Gölbaşı, Ankara, Turkiye
[f] Ankara University, Faculty of Sciences, Physics Department, Ankara 06100, Turkiye
[g] Center of Technology and Systems CTS/UNINOVA, School of Science and Technology, NOVA University Lisbon, Caparica, Portugal

ARTICLE INFO

Keywords:
YBCO superconductor powders
Polymers superconductor hybrid materials
Selfsustained drop-casting films
Levitation and magnetic properties
Surface and chemical analysis

ABSTRACT

Superconducting materials have been extensively studied for various applications, with YBCO alloys among the most researched and widely applied. This paper investigates the feasibility of using YBCO powder-based inks to produce cost-effective films with magnetic properties. Our studies demonstrate that levitation in liquid nitrogen is consistently observed in all fabricated films, regardless of ink composition or application method. Both drop-casting and spray-coating techniques were successfully employed to create levitating films. Additionally, various substrates—including aluminum foil (with and without adhesive), plastic foil, Teflon, and paper—were evaluated, with no significant impact on levitation performance. The levitation height was also compared to samples without a substrate. Depending on the binder, the resulting films exhibit rigidity or flexibility while maintaining their levitation capabilities even after multiple bending cycles. However, film conductivity is influenced by the binder type and concentration, which also affects the critical current density. A film with a thickness of 300 μm demonstrated a Jc of 2 kA/cm² at 65 K and zero magnetic field.

1. Introduction

Superconductor materials have faced extensive research after the demonstration that zero conductivity can be obtained at liquid nitrogen temperatures in cuprate alloys [1,2].

Among these YBCO (Yttrium Barium Copper Oxide) has emerged has one of the most thoroughly investigated and widely applied superconducting materials. This heightened interest stems from its remarkable properties, including high critical temperatures and critical magnetic fields, rendering it particularly promising for numerous practical applications. These applications span a broad spectrum, encompassing fields such as magnetically levitated transportation, magnetic resonance imaging (MRI), and energy systems [3,4].

Several techniques have been employed to produce YBCO alloys; while the solid-state reaction is commonly used for bulk materials [5], chemical vapour deposition (CVD), physical vapour deposition (PVD), pulsed laser deposition (PLD), ultrafast transient liquid assisted growth (UTLAG) techniques predominate in the production of second-generation high-temperature superconducting tapes [6–9]. In the recent years, novel high deposition rate techniques have emerged as potential candidates for reducing production costs while upholding material quality. These methods include aerosol-assisted spray pyrolysis [10], the photosensitive sol–gel method for patterned coatings [11], solution deposition via spin coating followed by pyrolysis and recrystallization [12,13], and single-deposition inkjet printing [14]. Furthermore, the advent of 3D printing technologies has presented promising avenues for YBCO fabrication albeit with their own sets of advantages and limitations [15–18].

The possibility to obtain flexible superconductor materials and devices have been demonstrated by recent works as examples: the inkjet production of stretchable superconducting micro/nano coils, circuits, and electrodes although using different material: droplets of GaInSn

* Corresponding author.
E-mail address: imf@fct.unl.pt (I. Ferreira).

https://doi.org/10.1016/j.nxmate.2025.100789
Received 21 May 2025; Accepted 30 May 2025
Available online 12 June 2025

[19]; patterned YBCO films have been grown on flexible nickel–tungsten substrates by a photosensitive sol–gel method [11,12]; a quasi-one-dimensional (Q1D) $Nb_2Pd_{0.73}S_{5.97}$ superconductor was produced on flexible paper by mechanical friction [20]; chemical exfoliation method was applied to create a stable, aqueous, surfactant-free, superconducting ink of 1 T′-WTe_2 that was printed to form a flexible film which is metallic at room temperature and superconducting below 7.3 K [21]; superconducting pastes using organic/inorganic hybrid compounds prepared with Nb or NbN superconducting particles were applied to form a large free-standing flexible film of length approximately 130 mm exhibiting superconductivity at 11 Kelvin [22].

In our study we present for the first time a low-cost composite consisting of YBCO powder and a polymeric binder forming a ink. This ink can be applied in any surface by painting or drop-casting, remains flexible as standalone film, and conforms to various shapes while exhibiting the levitation properties of YBCO 123 powder.

2. Experimental details

2.1. Production and evaluation of YBCO/Polymer films

YBCO/polymer films were produced using YBCO powder obtained by sintering a pre-mixture of Y_2O_3, $BaCO_3$, and CuO powders at 950 °C. The properties of the resulting powder have been previously published [15]. The sintered YBCO alloy was manually ground into a fine powder within an agata mortar, which was then used to prepare inks with various powder-to-binder weight ratios (p/b). The inks were applied using both spray-coating (with a mini-spray gun) and drop-casting (a homemade system utilizing a mask made from 0.3 mm thick tape) techniques to produce the films. During the spraying process, the environmental temperature was kept between 17 and 20 °C, with relative humidity ranging from 67 % to 70 %. For drop casting, a mixture of powder and binder solution was added to fully fill a 2 cm× 2 cm square mask made of tape, with a thickness of 0.3 mm, and let to dry at room temperature. The binder is a thermoplastic polyurethane (TPU) polymer. Film thickness was measured using a digital micrometer, and samples were weighed both with and without the substrate.

The quality of the films was assessed based on their levitation properties in liquid nitrogen. To recover the YBCO powder, the films were dissolved in the polymer solvent, and the powder was separated by removing both the polymer and solvent. This process was repeated through successive dissolutions until pure YBCO powder was obtained again. The entire process is illustrated in the diagram of Figure S1 and described in the supplementary information.

2.2. Properties analyses

Superconducting properties were measured using a vibrating sample magnetometer (VSM) of the Quantum Design physical property measurement system (PPMS) system. M–T curves were taken in a small measurement field of 50 Oe to determine the critical temperature Tc. J_c values were extracted from full hysteresis curves taken at a range of selected temperatures. The magnetic field was applied parallel to the cylindrical axis. XRD diffractograms were acquired in PANalytical X'Pert PRO with an X'Celerator detector using CuKα radiation at 45 kV and 40 mA in a Bragg–Brentano configuration. The XRD diffractograms were collected over the angular 2θ range 10°–90°, with a scanning step of 0.03°.

The SEM and EDS analysis was performed in a Scanning Electron Microscope-JEOL 6610 with Aztec analysis software.

The electric properties were measured on the top of the film with a four probe contacts using a Hall effect system with N_2 refrigeration (Hall Effect measurement system-Ecopia-HMS-7000) obtaining samples resistivity and mobility versus temperature. The Electrochemical impedance spectroscopy was performed in a Gamry potentiostate/galvanostate/ZRA 3000 equipment.

3. Results and discussion

The produced samples demonstrated levitation regardless of the substrates onto which the film was applicated: aluminium foil, aluminium foil with a glow, vinyl tape, and Teflon tape. All substrates were the same size (2 cm x2 cm), and the film had the same quantity of ink (2 g) corresponding to a thickness of ~ 300 μm; the weight variation depends on the weight of the substrate. Fig. 1 shows the levitation height, the duration of levitation at room temperature for the different substrates, and their respective weights. The samples were immersed in liquid nitrogen for 10 s, removed, and immediately placed on the top of the magnet.

Samples produced on Al foil due to its flexibility and mechanical resistance to manipulation were selected for magnetic characterization after removal of Al. This selection aimed to understand the influence of the film's processing methods, namely spray and drop-casting; the influence of the powder, whether prepared in the laboratory or sourced from a commercial piece, and the binder content. The results of magnetization shown in Fig. 2 indicate that a powder-to-binder weight ratio (p/b) of 0.6, using powder from a commercial damaged piece, results in homogeneous mixture of powder and binder, as observed in the SEM images and EDS analysis (supplementary information). This mixture exhibits a higher magnetization value at zero magnetic field, alongside a symmetric profile characteristic of diamagnetic properties, even at high temperatures (77 K and 65 K). This leads to observable Meissner effect, as evidenced by the magnetic levitation shown in the inset figure of the magnetization plot. Samples produced with laboratory-synthesised powder show different surface morphology. For p/b of 1.2, the films are formed by large agglomerates connected by the binder, whereas more uniform films are produced using both drop-casting and spray methods when a higher percentage of binder is used (p/b = 0.7). Although magnetic levitation is observed in all the samples, their magnetic properties differ in terms of profile and moment values as a function of the applied magnetic field.

The samples produced by using commercial YBCO powder exhibits the diamagnetic characteristic of superconductor, though the magnetization values for zero magnetic field are about one order of magnitude lower compared to the bulk films [23]. The ferromagnetic characteristics are seen in all the other samples at the temperatures analysed (77 K and 65 K). When compared with results obtained with similar YBCO powder used for 3D printed samples, we observe a similar behaviour, while the diamagnetic effect is observed at 10 K and 3.2 K, the ferromagnetic effect is seen at higher temperatures (77 K and 50 K) as well (Figure S1 supplementary information) [15]. Therefore, we may conclude that this effect is not related to the binder but rather to the YBCO powder used. The asymmetric magnetic hysteresis loops relative to the abscissa axis are typical of granular high-temperature-superconductors (HTSs) and are explained by the weak pinning of vortices in the surface layer of grains as reported by Balaev et al. [24]. The authors also discuss an interrelationship between the functional dependence of the magnetoresistance hysteresis width and the penetration of the field into the grains. The width of the magnetoresistance hysteresis is directly related to the compression of the magnetic flux in the inter grains region and the increase in the field induced by the magnetic moments of the HTS grains. The coexistence of ferromagnetism and superconductivity has also been observed in YBCO nanoparticles [25], suggesting that the local magnetic field produced by the spin-polarised moments is not strong enough to disrupt the enhanced superconducting pairs, allowing the spin-singlet superconductivity to withstand the local magnetic field. Other authors have attributed the observed asymmetric magnetic hysteresis loops in $LaCaBaCu_3O_7$ alloys to the presence of secondary phases that cause structural defects responsible for the irreversibility and remnant magnetization under an external field [26]. Indeed, the effect of grain and nano/micro particles in our case does not seem to induce ferromagnetism in samples produced with commercial powder. The homogeneity in size and composition

Aluminium foil	Aluminium foil w/glow	Vinyl tape	Teflon tape
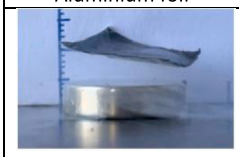	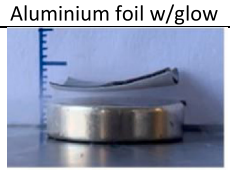		
0.5 cm; 6 s; 11 mg	0.3 cm; 7 s; 69 mg	0.3 cm, 4 s, 135 mg	0.5 cm, 7 s; 13 mg

Fig. 1. Images taken for films levitation and indication of measured levitation height, time, and weight, respectively.

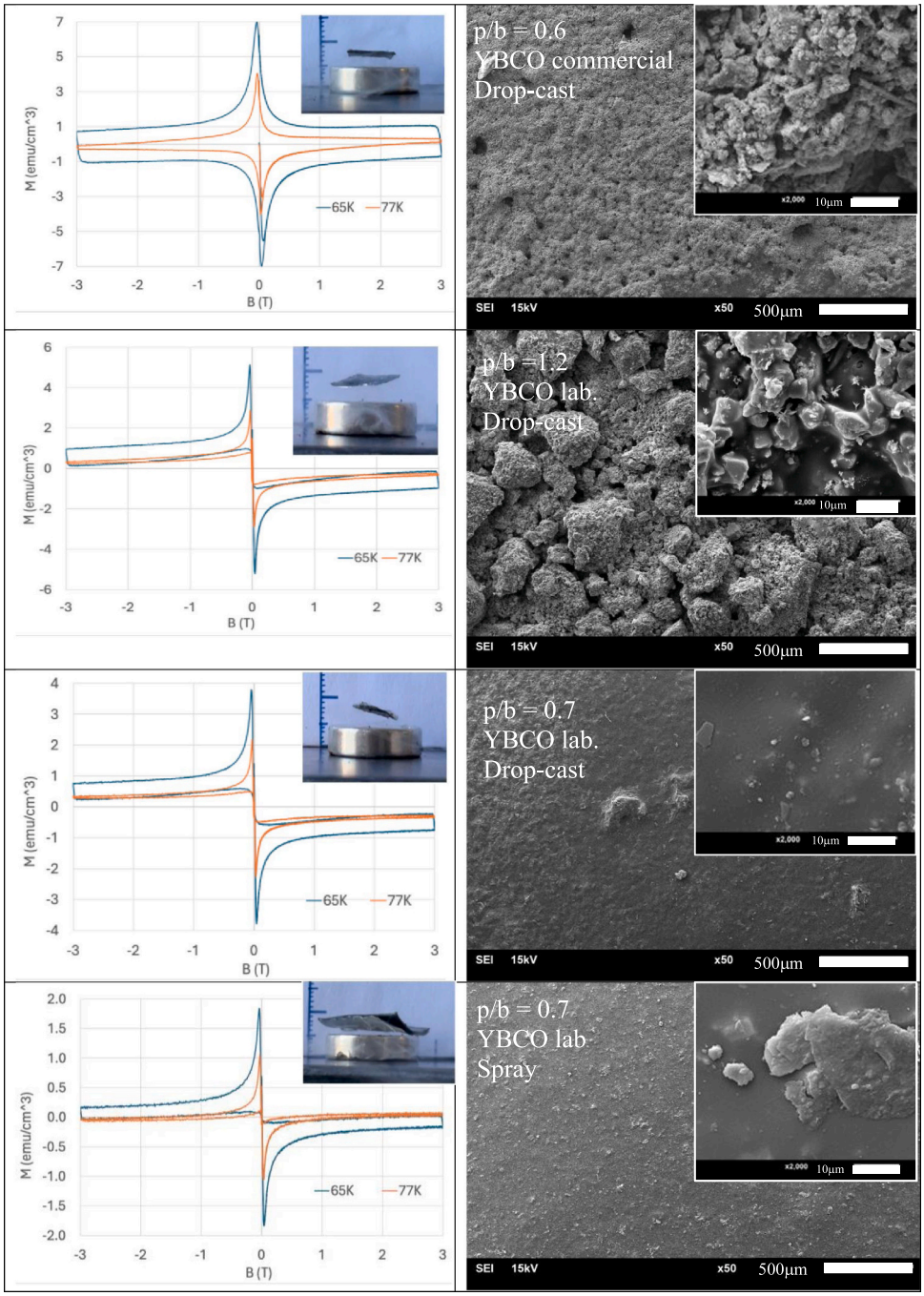

Fig. 2. Loop magnetization curves obtained for 77 K and 65 K, inset represents the magnetic levitation tests performed on the corresponding sample, and top view SEM images of the respective samples with two magnification x50 and x2000.

appears to be the main factor contributing to the perfect diamagnetism effect observed in hysteresis loop even at higher temperatures (77 K and 65 K) of powders obtained from commercial bulk YBCO parts. Considering the EDS analysis obtained at different micro spots on the analysed samples (supplementary information), we found that samples produced with commercial powder are quite uniform in terms of composition, whereas those with powder synthesized in the laboratory vary considerably, with some region rich in Ba and others in Cu. However, the XRD data (Figure 5S) indicates that the powder obtained in lab consists primarily of the YBCO 123 phase, and commercial powder contains a little percentage of YBCO 211 phase, as evidenced by three sequential peaks at 29–31° 2θ [27]. The presence of this minor YBCO 211 phase has been linked to an enhancement of the pinning phase [28]. As previously mentioned, the binder is not responsible for the asymmetric hysteresis loop of the magnetization, since the samples made with commercial YBCO powder contain a high quantity of binder and presents no hysteresis. The binder does restrict the current, as it is an insulating; the pathway for electron movement between grains is limited by the non-conductive material. Data of figure S3 in supplementary information an insulating typical behaviour of the resistance versus the frequency for samples with binder (Figure S3-A) and a conductive behaviour for the powder (Figure S3-B). The hall effect measurements done at room temperature also consolidate the results although the current measured is at DC. In the presence of liquid nitrogen, the samples exhibit an enhancement of the mobility, but resistivity is high, Table S1 in supplementary information. The presence of binder also impacts the critical current density, as observed in Fig. 3A. The low values of critical current density obtained can be attributed to the effect of polymeric binder, as well as the granular material and its impact on pinning dispersion, as verified by other authors [29–31]. However, these values are comparable to those obtained for porous samples produced by 3D printing about 340 A/cm^2 and 468 A/cm^2 for drop-casting films both at 78 K and same powder. The temperature dependence of the magnetic moment in the superconducting state has been measured under 50 Oe external magnetic field and it is shown in Fig. 3B. A variation in the critical temperature was observed, with Tc values of 93.1, 92.5, 90.8 and 92.9 K for samples A1, A5, A6 and A7, respectively. Therefore, the lowest Tc value (90.8 K) is obtained for drop-casting samples prepared with commercial powder and a p/b ratio of 0.6. The Tc for the samples is around 93 K. The slight difference may reflect the excess of oxygen in the samples containing the powder produced in the laboratory [32]. Other authors have observed that grain size has a remarkable influence on the critical temperature [33]. Tc of 94 K was also observed in previous work for 3D printed samples with similar powder [15].

The flexibility of the samples was tested by manually flexing them 20 times. Subsequently, the magnetic levitation was evaluated using the same procedure detailed in the experimental section (sample cooled in LN2 for 10 min, removed, and immediately placed on top of a magnet at room temperature). This sequence is illustrated in Fig. 4 and is complemented by a video in the supplementary information. Additionally, as shown in Figure S1 of the supplementary information, the damaged samples and polymer wastes with YBCO powder were collected and reused. The collected waste was immersed in the polymer solvent to dissolve the polymer, the powder sedimented and the liquid was removed. The powder obtained was used in the same manner as the new one, and the magnetic levitation was evaluated, as shown in Fig. 4.

4. Conclusions

The drop-casting and spray-coating methods for producing polymer/YBCO-powder composite films have been successfully demonstrated, with levitation properties observed regardless of the thin substrate on which they are deposited. The polyurethane binder provides flexibility, allowing the films to conform to curved surfaces and withstand folding.

Despite these advantages, the presence of the electrically insulating polymer limits the critical current density, resulting in lower values compared to bulk or ribbon superconductors, which restricts their application as superconductors. However, this study highlights the economic feasibility of the production process, the ability to recover YBCO powder for new film fabrication, and the straightforward recovery of used or damaged commercial bulk superconductors. These findings open new possibilities for flexible and cost-effective applications, including potential magnetic shielding.

Future studies will address the low conductivity by incorporating conductive inks as binders.

Author contributions

Beatriz Lucas carried out the experimental work under the supervision of Isabel Ferreira and Miguel Brito and contributed to the organization of data and writing of the document.

Miguel Brito was involved in the experimental work, samples preparation, supervision, and contributed to the writing of the document.

Canan Aksoy, was involved in the experimental SEM and EDS analyses, data analysis and contributed to the writing of the document.

Bakiye Cakir, Elvan Coşkun, Ali Gencer, were involved in the acquisition and analysis of magnetic data, as well as in writing the paper.

Anabela Pronto and Isabel Ferreira supervised the work were involved in all aspects of data compilation, analysis, and paper writing.

Funding

This work was financed by national funds from FCT—Fundação para a Ciência e a Tecnologia, I.P. projects LA/P/0037/2020 of the Associate Laboratory Institute of Nanostructures, Nanomodelling and Nanofabrication—i3N. This work was also supported by ERC-CoG-2014, CapTherPV, 647596.

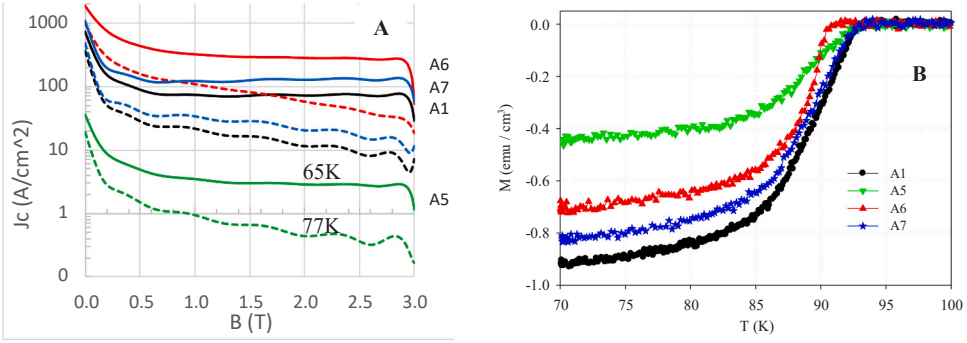

Fig. 3. A - magnetic field dependence of the critical current density (Jc) from magnetization measurements (solid line corresponds to 77 K and dashed line to 65 K). B- magnetic moment versus temperature variation under an external 50 Oe magnetic field. Samples A6 (p/b=0.6 commercial powder; drop-cast), A7 (p/b=1.2 lab powder; drop-cast), A1 (p/b=0.7 lab powder; drop-cast), A5 (p/b=0.7 lab powder; spray).

Fig. 4. A: images showing rolled-up samples and magnetic levitation with both curved and flat samples (scale: 1 cm between large lines). B: magnetic levitation performed on samples produced with powder waste generated in this study.

Declaration of Competing Interest

The authors declare that they have no known competing financial interests or personal relationships that could have appeared to influence the work reported in this paper.

Appendix A. Supporting information

Supplementary data associated with this article can be found in the online version at doi:10.1016/j.nxmate.2025.100789.

References

[1] J.G. Bednorz, K.A. Muller, Possible hight c superconductivity in the BaLaCuO system, Z. Phys. B Condens. Matter 64 (2) (1986) 189–193, https://doi.org/10.1007/BF01303701.
[2] M.K. Wu, et al., Superconductivity at 93 k in a new mixed-phase Y-Ba-Cu-O compound system at ambient pressure, Phys. Rev. Lett. 58 (9) (1987) 908–910, https://doi.org/10.1103/PhysRevLett.58.908.
[3] C. Yao, Y. Ma, Superconducting materials: challenges and opportunities for large-scale applications, iScience 24 (6) (2021) 102541, https://doi.org/10.1016/j.isci.2021.102541.
[4] H.-U. Habermeier, Science and technology of cuprate-based high temperature superconductor thin films, heterostructures and superlattices—the first 30 years (Review Article), Low. Temp. Phys. 42 (10) (2016) 840–862, https://doi.org/10.1063/1.4965889.
[5] D.K. Namburi, Y. Shi, D.A. Cardwell, The processing and properties of bulk (RE) BCO high temperature superconductors: current status and future perspectives, Supercond. Sci. Technol. (2021), https://doi.org/10.1088/1361-6668/abde88.
[6] K. Wang, et al., Advances in second-generation high-temperature superconducting tapes and their applications in high-field magnets, Soft Sci. 2 (3) (2022) 12, https://doi.org/10.20517/ss.2022.10.
[7] D.-X. Wang, J. Chen, D.-F. Zhou, C.-B. Cai, Development of metal-organic deposition-derived second-generation high-temperature superconductor tapes and artificial flux pinning, Adv. Manuf. 11 (3) (2023) 523–540, https://doi.org/10.1007/s40436-023-00447-z.
[8] C. Park, et al., Long length fabrication of YBCO on rolling assisted biaxially textured substrates (RABiTS) using pulsed laser deposition, IEEE Trans. Appl. Supercond. 9 (2) (1999) 2276–2279, https://doi.org/10.1109/77.784924.
[9] S. Rasi, et al., Kinetic control of ultrafast transient liquid assisted growth of solution-derived $YBa_2Cu_3O_7$ -x superconducting films, Adv. Sci. 9 (32) (2022) 2203834, https://doi.org/10.1002/advs.202203834.
[10] B.-J. Kim, et al., Deposition of YBCO thin film by aerosol assisted spray pyrolysis using Nitrates', IEEE Trans. Appl. Supercond. 21 (3) (2011) 2937–2940, https://doi.org/10.1109/TASC.2010.2091931.
[11] L. Li, G. Zhao, L. Lei, F. Yan, B. Deng, C. Li, Fine patterned YBCO films grown on flexible nickel–tungsten substrates by photosensitive sol–gel method, Mater. Res. Bull. 147 (2022) 111631, https://doi.org/10.1016/j.materresbull.2021.111631.
[12] L. Saltarelli, et al., Metal propionate solutions for High-Throughput Liquid-Assisted manufacturing of superconducting $REBa_2Cu_3O_{7-\delta}$ (RE = Y, Gd, Sm, and Yb) films, ACS Appl. Mater. Interfaces 16 (40) (2024) 54199–54214, https://doi.org/10.1021/acsami.4c11685.
[13] I. Bretos, et al., Solution-derived $YBa_2cu_3o_{7-\delta}$ (YBCO) superconducting films with $BaZrO_3$ (BZO) nanodots based on reverse micelle stabilized nanoparticles, J. Mater. Chem. C. 3 (16) (2015) 3971–3979, https://doi.org/10.1039/C4TC02543A.
[14] B. Villarejo, et al., High performance of superconducting $YBa_2cu_3o_7$ thick films prepared by Single-Deposition inkjet printing, ACS Appl. Electron. Mater. 3 (9) (2021) 3948–3961, https://doi.org/10.1021/acsaelm.1c00513.
[15] D. Mendes, et al., Low-cost and high-performance 3D printed YBCO superconductors, Ceram. Int. 47 (1) (2021) 381–387, https://doi.org/10.1016/j.ceramint.2020.08.143.
[16] X. Wei, R.S. Nagarajan, E. Peng, J. Xue, J. Wang, J. Ding, Fabrication of YBa2Cu3O7−x (YBCO) superconductor bulk structures by extrusion freeforming, Ceram. Int. 42 (14) (2016) 15836–15842, https://doi.org/10.1016/j.ceramint.2016.07.052.
[17] X. Wei, E. Peng, Y. Xie, J. Xue, J. Wang, J. Ding, Extrusion printing of a designed three-dimensional $YBa_2cu_3o_{7-x}$ superconductor with milled precursor powder, J. Mater. Chem. C. 5 (13) (2017) 3382–3389, https://doi.org/10.1039/C6TC05393A.
[18] P. Pęczkowski, et al., Structural, magnetic, and thermal properties of 3D-printed porous Y-Ba-Cu-O superconductors, p. S0955221924003157, J. Eur. Ceram. Soc. (2024), https://doi.org/10.1016/j.jeurceramsoc.2024.04.009.
[19] L. Ren, et al., Nanodroplets for stretchable superconducting circuits, Adv. Funct. Mater. 26 (44) (2016) 8111–8118, https://doi.org/10.1002/adfm.201603427.
[20] P. Zhan, Z. Wang, Y. Liu, J. Wang, Y. Xing, Integrating quasi-one-dimensional superconductors on flexible substrates, AIP Adv. 12 (6) (2022) 065319, https://doi.org/10.1063/5.0096973.
[21] X. Song, et al., Synthesis of an aqueous, air-stable, superconducting $1T'$-WS_2 monolayer ink, Sci. Adv. 9 (12) (2023) eadd6167, https://doi.org/10.1126/sciadv.add6167.
[22] H. Takashima, Y. Yoshida, M. Furuse, Superconducting flexible organic/inorganic hybrid compound adhesives, ACS Omega 7 (50) (2022) 47405–47410, https://doi.org/10.1021/acsomega.2c06977.
[23] A.K. Jha, N. Khare, R. Pinto, Influence of interfacial LSMO nanoparticles/layer on the vortex pinning properties of YBCO thin film, J. Supercond. Nov. Magn. 27 (4) (2014) 1021–1026, https://doi.org/10.1007/s10948-013-2384-0.
[24] D.A. Balaev, S.V. Semenov, D.M. Gokhfeld, New evidence of interaction between grain and boundaries subsystems in granular High-Temperature superconductors, J. Supercond. Nov. Magn. 34 (4) (2021) 1067–1075, https://doi.org/10.1007/s10948-021-05812-2.
[25] Z. Zhu, et al., Coexistence of ferromagnetism and superconductivity in YBCO nanoparticles, Phys. Chem. Chem. Phys. 14 (11) (2012) 3859, https://doi.org/10.1039/c2cp23046a.
[26] L.D.L. Santos V, et al., Magnetic properties of the superconductor LaCaBaCu3O7', Open Supercond. J. 2 (1) (2010) 19–27, https://doi.org/10.2174/1876537801002010019.
[27] J. Sklenka, O. Jankovský, T. Hlásek, F. Antončík, Novel chemical recycling process of REBCO materials showcased on TSMG-processed waste, J. Mater. Chem. C. 12 (9) (2024) 3326–3332, https://doi.org/10.1039/D3TC01729J.
[28] V. Bartůněk, J. Luxa, D. Sedmidubský, T. Hlásek, O. Jankovský, Microscale and nanoscale pinning centres in single-domain REBCO superconductors, J. Mater. Chem. C. 7 (42) (2019) 13010–13019, https://doi.org/10.1039/C9TC01455A.
[29] T. Sueyoshi, Modification of critical current density anisotropy in high-Tc superconductors by using Heavy-Ion irradiations, Quantum Beam Sci. 5 (2) (2021) 16, https://doi.org/10.3390/qubs5020016.
[30] R.O. Rezaev, E.I. Smirnova, O.G. Schmidt, V.M. Fomin, Topological transitions in superconductor nanomembranes under a strong transport current, Commun. Phys. 3 (1) (2020) 144, https://doi.org/10.1038/s42005-020-00411-4.
[31] E. Rivasto, et al., Self-assembled nanorods in YBCO matrix – a computational study of their effects on critical current anisotropy, Sci. Rep. 10 (1) (2020) 3169, https://doi.org/10.1038/s41598-020-59879-3.
[32] A.M. Ali, A. Sedky, H. Algarni, M.A. Sayed, Argon annealing and oxygen purity affect structural and critical parameters of YBCO copper oxide system, J. Low. Temp. Phys. 197 (5–6) (2019) 445–457, https://doi.org/10.1007/s10909-019-02234-2.
[33] S.K. Hasanain, N. Akhtar, A. Mumtaz, Particle size dependence of the superconductivity and ferromagnetism in YBCO nanoparticles, J. Nanopart. Res. 13 (5) (2011) 1953–1960, https://doi.org/10.1007/s11051-010-9947-9.